Volume 7, Issue 1, 2017, 1896 - 1900 ISSN 2069-5837

Biointerface Research in Applied Chemistry

www.BiointerfaceResearch.com

Original Research Article Open Access Journal

Received: 11.12.2016 / Revised: 27.01.2017 / Accepted: 10.02.2017 / Published on-line: 15.02.2017

Synthesis, characterization and photocatalytic activity of β-Bi_2O_3 nanomaterial via degradation of Orange II under visible light irradiation

Mohamed Badaoui [1, 2, *], Messaoud Chaib [1], Ana Rey Barroso [3], Belkacem Ziane [2]

[1] Department of Chemistry, Faculty of Sciences of the Matter, IbnKhaldoun University of Tiaret, BP78, Zaaroura, Tiaret, Algeria

[2] Department of Chemistry, Faculty ofExact Sciences, DjilaliLiabesUniversty, BP89 City El Arbi Ben m' hidiSidiBelAbbés, Algeria

[3] Departamento de IngenieríaQuímica y QuímicaFísica, Universidad de Extremadura, Av. Elvas s/n, 06006 Badajoz, Spain

*corresponding author e-mail address: ***bm_med17@yahoo.fr***

ABSTRACT

In this paper, the hydrothermal synthesis technique was used to produce β-Bi_2O_3 sample. Visible light has been chosen as a more efficiently adapted in photocatalytic reactions for this kind of material. Several investigations have been done in this study; the X-ray photoelectron spectroscopy (XPS) showed the chemical composition of the sample, the microstructural features of our synthesized material were characterized by X-ray diffraction (XRD), another set of properties have been studied using the Brunauer–Emmett–Teller (BET), Diffuse reflectance UV–vis spectroscopy (DR-UV–vis) and The pH of the point of zero charge (pH_{PZC}). The photocatalytic activity of our prepared catalyst was found by the degradation of Orange II (OII) aqueous solutions under visible light irradiation. The effect of operational parameters such as amount of catalyst, initial solution pH, Hydrogen peroxide (H_2O_2), and the initial concentration of OII were investigated.

Keywords: *PhotocatalyticActivity, Visible Light, Bismuth Oxide, Orange II.*

1. INTRODUCTION

Photocatalytic degradation of environmental pollutants in water and/or air by semiconducting materials has attracted extensive attentions during recent 20 years [1]. The basic process of photocatalysis consists in ejecting an electron from the valence band (VB) to the conduction band (CB) of the semi-conductor thus creating a hole (h+) in the valence band. This is followed by the formation of extremely reactive radicals such as .OH at the semiconductor surface or by direct oxidation of the polluting species by h+. As for the ejected electrons, they react with electron acceptors such as adsorbed oxygen or dissolved in water. Many different semiconductors, such as, TiO_2, SnO_2, WO_3, Bi_2O_3, ZnO , Fe_2O_3, CdS, ZnS, and $SrTiO_3$, have been used as photocatalysts for the photodegradation of organic or inorganic pollutants [2–9]. Bismuth oxide (Bi_2O_3) has only recently gained interest [10]. It has many application such as optical coatings, microelectronics, ceramic glass, gas sensor, fuel cells, photocatalysts, etc[11-16], and also more crystalline phases, which are α-Bi_2O_3, β-Bi_2O_3, γ-Bi_2O_3 and δ-Bi_2O3 [16, 17]. Bi_2O_3 has excellent physical and chemical properties, including good visible-light responsive [18-20]. Furthermore, the band gap energy are 2.85 eV and 2.58 eV for α-Bi_2O_3 and β-Bi_2O_3 respectively [21, 22], which is a fundamental prerequisite for suitable application as photocatalyst for water purification [23]. In this work, β-Bi_2O_3 powder was synthesized by hydrothermal method and characterized by using techniques such as X-ray diffraction (XRD), X-ray photoelectron spectroscopy (XPS), and Diffuse reflectance UV–vis spectroscopy (DR-UV–vis), Brunauer–Emmett–Teller analysis (BET). Photocatalytic activity of catalyst was evaluated by measuring the photodegradation of Orange II under visible light irradiation. The effect of different operating conditions, such as catalyst loading, pH, H_2O_2, initial concentrations of OII, and addition of Hydrogen peroxide (H_2O_2) were also studied.

2. EXPERIMENTAL SECTION

2.1. Catalyst Preparation. The β-Bi_2O_3 catalyst was prepared by hydrothermal process [18]. In detail, 2 mmol of $Bi(NO_3)_3$, $5H_2O$ was dissolved in 10 ml of HNO_3 (1M), and then 1.5 mmol of citric acid was added to the solution under agitation. After 10 min, the pH value of the clear solution was adjusted to 4 with the addition of NaOH (1M) and transferred into a Teflon-lined stainless steel autoclave and maintained at 180°C for 24 h. After cooling, the precipitate was separated by centrifugation, washed with pure water and ethanol absolute, and dried at 80°C for 12h. The prepared powder was calcined at 350°C for 3h to produce β-Bi_2O_3 nanoparticles.

2.2. Characterizations. The crystalline phases present in the catalyst was inferred from their X ray diffraction (XRD) patterns recorded using a powder Bruker D8 Advance XRD diffractometer with a CuKα radiation (λ=0.1541 nm).The data were collected from 2θ=10° to 70°. Crystalline composition semi-quantitative analysis of the samples was performed on multi-phase patterns by the Reference Intensity Ratio (RIR) method using reference diffraction patterns by means of EVA v.14 software (Bruker-AXS). BET surface area and pore volume of the photocatalyst was determined from their nitrogen adsorption–desorption isotherms obtained at-196 1C using an Autosorb 1 apparatus (Quanta-chrome). Prior to analysis the samples were outgassed at 150°C for 24 h under high vacuum ($<10^{-4}$ Pa). X-ray photoelectron spectra (XPS) were obtained with a Kα Thermo Scientific apparatus with an Al Kα (hν=1486.68 eV) X-ray source using a

voltage of 12 kV under vacuum (2×10^{-7} mbar). Diffuse reflectance UV–vis spectroscopy (DR-UV–vis) measurements, useful in the determination of the semiconductor band gap, were performed with an UV–vis-NIR Cary 5000 spectrophotometer (Varian-Agilent Technologies) equipped with an integrating sphere device.

2.3. photocatalytic activity measurements

Thephotocatalytic activity under visible light irradiation of the β-Bi_2O_3 catalyst was evaluated by using Orange II solution at ambient temperature. The irradiation experiments were carried out in the photoreactor with a 250 mL Flask (Pyrex glass) and visible LED lamps as light source under continuous stirring. Before each irradiation, the mixtures were sonicated for 5 min in order to disperse the catalyst, and the suspension was kept in the dark for 30 min in order to reach the adsorption equilibrium. For reactions in different pH media, the initial pH of the suspensions was adjusted by addition of either NaOH (0.1N) or HCl(0.1N) solutions. Before analysis, each sample was filtered through a 0.45µm Whatman filter to eliminate the β-Bi_2O_3 particles. During the photocatalytic test, 5 ml of the solution were extracted at given irradiation time intervals and analyzed by UV–vis spectrophotometer (λ max = 484 nm).

3. RESULTS SECTION

3.1. Characterization of the photocatalyst. The powder X-ray diffraction (XRD) pattern provides crystallinity and phase structures information for the catalyst. **Fig. 1** shows the XRD patterns of β-Bi_2O_3 powder. The diffraction peaks can be indexed as pure β-Bi_2O_3 structure with the major peaks at 2θ: 27.7, 31.1, 32.4, 45.7, 45.6, 53.4, 55.1, and 57.2, corresponding, respectively, to the diffractions of the (201), (002), (220), (222), (400), (203), (421), and (403) plane of the tetragonal β-Bi_2O_3[24].The average crystal size of the β-Bi_2O_3 powder was calculated by the Debye-Scherrer equation [25]:

$$D = \frac{0.9\lambda}{\beta \cos\theta} \quad \text{(I)}$$

Where λ is the wavelength of Cu Ka radiations (1.54A°), β the full width at half-maximum of the peak corresponding to the plane **(201)**, and h the angle obtained from 2θ value corresponding to maximum intensity peak in XRD pattern. The diameter of crystallite size of synthesized β-Bi_2O_3 powder was 124 nm. The BET surface area of the β-Bi_2O_3 is 3.2 m^2/g.

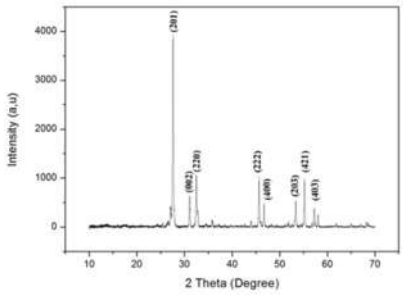

Figure 1. XRD spectra of β-Bi_2O_3.

High-resolution XPS was used to elucidate the detailed surface chemical compositions and their electronic states of the catalyst.

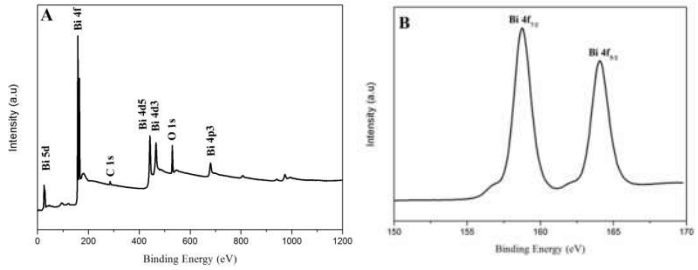

Figure 2. XPS survey spectrum of Bi (A) and the high-resolution XPS spectra of Bi 4f region (B).

Figure 2 shows the XPS spectra of β-Bi_2O_3 , the XPS signals of Bi 4f were observed at binding energies at 164.08 eV (Bi 4f5/2) and 158.76 eV (Bi 4f7/2) ascribed to $Bi^{3+}$from XPS analysis, which is consistent with the previous reports of β-Bi_2O_3 powders [26]**.** The optical property (Eg) of the β-Bi_2O_3 was measured by the diffuse reflectance spectra using the Munk-Kubelka function [27]:

$$F(R) = \frac{(1-R)^2}{2R} = \frac{k}{s} \quad \text{(II)}$$

R = (I/Io) diffuse is the diffuse reflectivity from an infinitely thick layer (about 2-3 mm) and k the absorptivity (cm^{-1}), the scattering factor (s) is independent of the wavelength for particle sizes larger than the wavelength of the light. The gap Energy (Eg) is determined by extrapolating the linear portion of the curve $(F(R)\times(h\upsilon))^2$ to hυ axis as showed in **Fig.3**;has been found to 2.55 eV . These values can be compared with band gap values cited in the literature [21, 22].

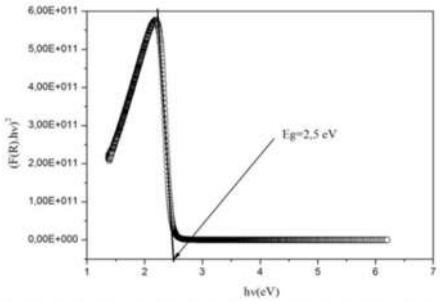

Figure 3. UV–vis diffuse reflectancespectra of β-Bi_2O_3.

The pH of the point of zero charge it is a parameter very important in the photocatalytic activity was determined by the method "pH drift"**[**28] .**Fig. 4** show the pH_{PZC} determination of the β-Bi_2O_3. The pH_{PZC} is the point where the curve of pH_{final}vs$pH_{initial}$ intersects the line $pH_{initial}$=pH_{final}, with the value for the β-Bi_2O_3 is 9.2.

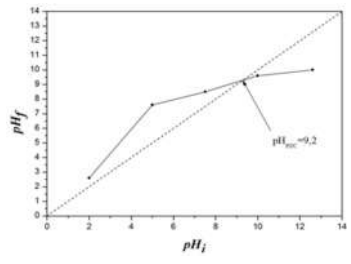

Figure 4. pHPZC determination of the β-Bi_2O_3.

3.2. Photocatalytic activity of the β-Bi_2O_3 catalyst. The photocatalytic degradation of 20mg of OII solution containing 0.1 g L^{-1} β-Bi_2O_3 as function of irradiation time under varied conditions are illustrated in **Figure 5**. The result of this study show a negligible decrease of the OII under irradiation in the absence of β-Bi_2O_3 from the direct photolysis of the OII solution .in the presence of β-Bi_2O_3 without a light source Slight loss was observed due to the adsorption of OII on the surface of β-Bi_2O_3. The irradiation under visible light in the presence of catalyst caused 56% degradation of OII in 120 min.

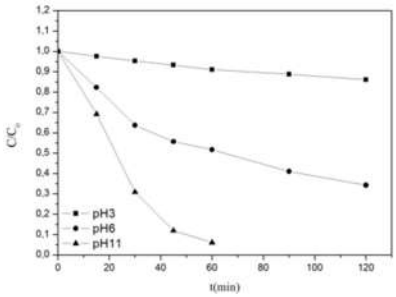

Figure 5. Photocatalytic degradation of OII as a function of irradiation time [β-Bi_2O_3]=1.0 g/L, [OII]=15mg/L.

3.3. Effect of initial pH. The solution pH appears to play an important role in the photocatalytic degradation of various pollutants [29, 30]. The pH of the solution is adjusted before irradiation **Fig. 6** show the degradation of OII with irradiation time for different pH values. The degradation efficiency increases with increase in pH from 3 to 11.The zero-point charge for β-Bi_2O_3 is 9.2. Above this pH value β-Bi_2O_3 surface is negatively charged by means of adsorbed OH^- ions. The presence of large quantities of OH^- ions on the particle surfaces as well as in the reaction medium favors the formation of OH•. So the optimum pH for efficient OII removal is pH =11. The optimum pH 11 was also reported for the photodegradation of reactive azo dye [29, 30].

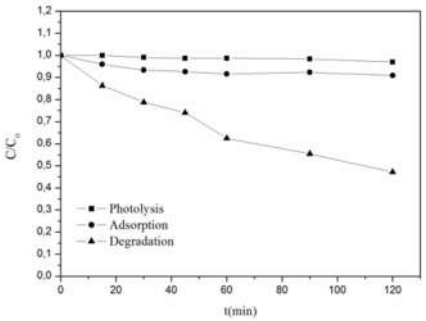

Figure 6. Effect of pH on degradation of OII. [OII] = 10mg/L, β-Bi_2O_3= 1 g/L.

3.4. Effect of H_2O_2. The addition of an oxidant into a catalyst suspension has been proven to improve the photodegradation of the organic compound [31-33]. **Fig.7** shows the effect of adding 37.5 µL of H_2O_2 on the degradation of OII. After 120 min reaction time, the degradation efficiency has increased to about 85% when H_2O_2 was added, while it did not exceed 56% if the reaction proceeds without H_2O_2. This increase is expected, because of the high oxidizing capacity of hydroxyl radicals, which are produced from H_2O_2 by the following degradation mechanism [34]:

$$H_2O_2 \rightarrow 2OH^{\bullet}$$
$$H_2O_2 + O_2^- \rightarrow OH^{\bullet} \rightarrow OH^- + O_2$$
$$H_2O_2 + e^- \rightarrow OH^{\bullet} + OH^-$$

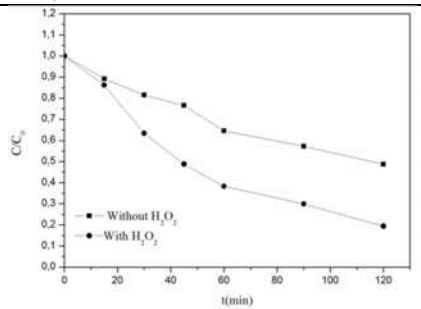

Figure 7. Effect of addition of H_2O_2.[OII] = 15 mg/L; [β-Bi_2O_3] = 1g/L; H_2O_2 =37.5µL.

3.5. Effect of the amount of catalyst. The amount of catalyst is an important parameter. Hence, the effect of catalyst concentration on the degradation of the OII was investigated by using different concentrations of β-Bi_2O_3 ranging from 0.5 to 2.0 g /Las **Fig. 8** shows. The degradation of the OII increase This can be explained in terms of availability of active sites on the catalyst surface and the penetration of Visible light into the suspension [35], and then decrease with the increase in the catalyst concentration due to the reduction of the penetration of visible light within the irradiated solution [36, 37]. Hence, the optimum amount of catalyst for photocatalytic degradation of OII was found to be 1.0 g/L.

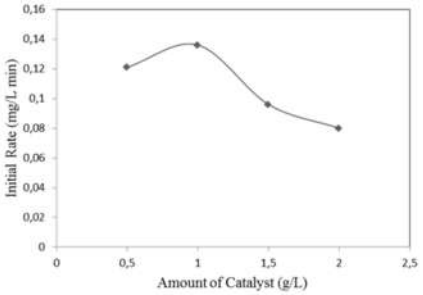

Figure 8. Effect of β-Bi_2O_3 Amount. [OII]= 10 mg/L.

3.6. Effect of initial concentration and kinetic study of OII. The initial concentration of reactant plays an important role on the photocatalytic degradation of organic compounds [38]. **Fig. 9** shows the degradation of OII as a function of time for different initial concentrations. It is observed the degradation of OII decreases with increase in OII concentration from 5mg/L to 25mg/L .Similar results have been reported for the photocatalytic oxidation of other dyes [39, 40].When the OII concentration increases the amount of OII adsorbed on the catalytic surface increases. This affects the photocatalytic activity of β-Bi_2O_3. The increase in OII concentration also decreases the path length of photon entering into the OII solution. At high concentration of dye, the dye molecules may absorb a significant amount of light rather than the catalyst and this may also reduce the catalytic efficiency [41].

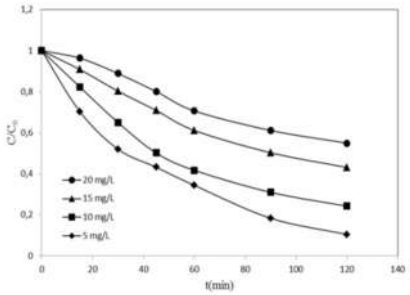

Figure 9. Effect of initial concentration of OII on the photocatalytic degradation under Visible light irradiation.

The kinetic modeling of the photocatalytic degradation of many organic compounds followed the Langmuir-Hinshelwood model (L-H model), which also covers the adsorption properties of the substrate on the photocatalyst surface [42].This model, developed by [43, 44], is expressed by the equation:

$$r = -\frac{dC}{dt} = K_{app}\, C \quad \text{(III)}$$

Where r is the degradation rate (mg/L min), Kapp the apparent constant of degradation (1/min), C is the concentration of the organic substrate at any time t (mg/L).

The integration of this equation (with limitation: $C=C_0$ for t =0) leads to the following equation:

$$Ln\frac{C_0}{C} = K_{app}t \quad \text{(IV)}$$

The kinetic of degradation of OII at different concentrations is respectively illustrated in **Fig 10**. The photocatalytic degradation of OII by β-Bi_2O_3 obeys pseudo-first-order kinetics. At low initial OII concentration the rate expression is given by equation (IV), the apparent constant (k_{app}) decreased with the increasing of concentration of OII , The correlation constant for the fitted line and the rate constants are calculated and their values are grouped in **Table 1**.

Table 1. Rate constant values for the degradation of OII.

C_i (mg/L)	R^2	K_{app}
5	0.9954	0.0188
10	0.9801	0.0095
15	0.9898	0.0039
20	0.9982	0.0024

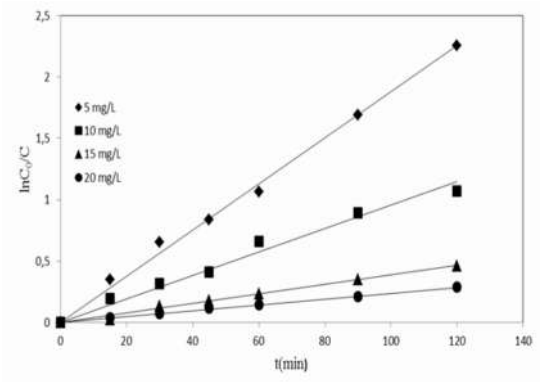

Figure 10. Kinetic fit for the degradation of OII with β-Bi_2O_3.[β-Bi_2O_3] = 1.0 g /L; pH = 6.

4. CONCLUSIONS

In this study, the β-Bi_2O_3 catalyst was prepared by hydrothermal process. The characteristic patterns of XRD, XPS, BET and UV–Vis–DRS displayed that the catalyst has better crystallization, smaller crystal size, and stronger response to visible light. The obtained catalyst was used as photocatalyst for the degradation of OII aqueous solutions under visible light irradiation. The result of photocatalytic activity of β-Bi_2O_3 was very efficient under visible light irradiation.The optimum operational parameters for the photocatalytic degradation of OII solution at ambient temperature were determined to be: β-Bi_2O_3 concentration 1 g/L, initial pH is 11 and the additions of H_2O_2 enhance the OII removal process. It can be seen also that the photocatalytic degradation follows a first-order kinetics and Langmuir–Hinshelwood behaviour.

5. REFERENCES

[1] M.R. Hoffmann, S.T. Martin, W. Choi, D.W. Bahnemann, Environmental Applications of Semiconductor Photocatalysis, *Chemical Reviews*. 95, **1995**.

[2] A.E.H. Machado, A.J. Gomes, C.M.F. Campos, et al., Photoreactivity of lignin model compounds in the photobleaching of chemical pulps 2. Study of the degradation of 4-hydroxy-3-methoxy-benzaldehyde and two lignin fragments induced by singlet oxygen , *Journal of Photochemistry and Photobiology A: Chemistry*, 110, 1, 99, **1997** .

[3] A. Hagfeldt, M. Graetzel, Light-Induced Redox Reactions in Nanocrystalline Systems , *Chemical Reviews*., 95, 1, 49, **1995**.

[4] M. Schiavello, Some working principles of heterogeneous photocatalysis by semiconductors, *Electrochimica Acta* , 38, 1, 11, **1993**.

[5] H. Hidaka, J. Zhao, E. Pelizzetti, N. Serpone, Photodegradation of surfactants. 8. Comparison of photocatalytic processes between anionic DBS and cationic BDDAC on the titania surface , *Journal of Physical . Chemical* , 96, 5, 2226, **1992**.

[6] R.W. Matthews, Photocatalytic oxidation and adsorption of methylene blue on thin films of near-ultraviolet-illuminated TiO_2, *Chemical Society Faraday Transactions1*, 85, 6, 1291, **1989**.

[7] S. Lakshmi, R. Renganathan, S. Fujita, Study on TiO_2-mediated photocatalytic degradation of methylene blue , *Journal of Photochemistry and Photobiology A: Chemistry* 88, 2-3, 163, **1995**.

[8] B. Singhal, A. Porwal, A. Sharma, R. Ameta, S.C. Ameta, Photocatalytic degradation of cetylpyridinium chloride over titanium dioxide powder, *Journal of Photochemistry and Photobiology A: Chemistry*, 108, 1, 85, **1997**.

[9] N. Serpone, P. Maruthamuthu, P. Pichat, E. Pelizzetti, H. Hidaka, Exploiting the interparticle electron transfer process in the photocatalysed oxidation of phenol, 2-chlorophenol and pentachlorophenol: chemical evidence for electron and hole transfer between coupled semiconductors, *Journal of Photochemistry and Photobiology A: Chemistry*, 85, 2, 247, **1995**.

[10] M.L. Zhang, T.C. An, X.H. Hu, C. Wang, G.Y. Sheng, J.M. Fu, Preparation and photocatalytic properties of a nanometer ZnO–SnO_2 coupled oxide, *Applied CatalysisA: General,* 260, 2, 215, **2004**.

[11] H. Kim, C. Jin, S. Park, W.I. Lee, I.J. Chin, C.M. Lee, Chem, Structure and optical propertiesof $Bi_2S_3$and Bi_2O_3 nanostructures synthesized via thermal evaporation and thermal oxidation routes, *Chemical Engineering Journal*, 215-216, 151, **2013**.

[12] D.G. Collins, K.I. Arshak, A study of composite Bi_2O_3, In_2O_3 and RuO_2 planar thick film piezoresistive gauges, *Microelectronics Journal*, 27, 1, 59, **1996**.

[13] S.F. Song, Z.Y. Wen, Y. Liu, Development and characterizations of Bi_2O_3-containing glass–ceramic sealants for sodium sulfur battery, Journal of Non-Crystalline Solids , 375, 25, **2013**.

[14] Y.C. Zhou, Z.C. Zhang, C. Yuan, J.L. Li, C.R. Xia, Z.L. Zhan, S.R. Wang, Metal-supported solid oxide fuel cells with in-situ sintered $(Bi_2O_3)_{0.7}(Er_2O_3)_{0.3}$-Ag composite cathode, *International Journal of Hydrogen Energy*, 38, 36, 16579, **2013**.

[15] D.P. Dutta, M. Roy, A.K. Tyagi, Dual function of rare earth doped nano Bi_2O_3: white light emission and photocatalytic properties , *Dalton Transaction,* 41, 34, 10238, **2012**.

[16] A. Cabot, A. Marsal, J. Arbiol, J.R. Morante, Bi_2O_3 as a selective sensing material for NO detection, Sensors and Actuators B: Chemical, 99, 1, 74, **2004**.

[17] G.Q. Zhu, J. Zhang, Synthesis and photocatalytic performance of Ag-loaded β-Bi_2O_3 microspheres under visible light irradiation , *Journal of Alloys and Compounds*, 509, 39, 9479, **2011**.

[18] G.H. Zhong, J.L. Wang, Z. Zeng, Ionic transport properties in doped β-Bi_2O_3, *Journal of Physics Conference Series*, 29, 1, 106, 2006.

[19] V. Fruth, M. Popa, D. Berger, R. Ramer, M. Gartner, A. Ciulei, Deposition and characterisation of bismuth oxide thin films , Journal of the European Ceramic Society , 25, 12, 2171, **2005**.

[20] H.T. Fan, X.M. Teng, S.S. Pan, C. Ye, G.H. Li, L.D. Zhang, Optical properties of β-Bi2O3 thin film grown by reactive sputtering , *Applied Physical Letter*, 87, , 231916, **2005**.

[21] Leontie L, Caraman M, Alexe M, Harnagea C, Structural and optical characteristics of bismuth oxide thin films, *Surface Science*, 507-510, 480, **2002**.

[22] Fruth V, Popa M, Berger D, Ramer R, Gartner M, Ciulei A, Zaharescu M, Deposition and characterisation of bismuth oxide thin films, *Journal of the European Ceramic Society*, 25, 12, 2171, **2005**.

[23] A. Hameed, T. Montini, V. Gombac, P. Fornasiero, Surface Phases and Photocatalytic Activity Correlation of Bi_2O_3/Bi_2O_{4-x} Nanocomposite, *J.American chemical society*, 130, 9658, **2008**.

[24] Hou J, Yang C, Wang Z, Zhou W, Jiao S, Zhu H , In situ synthesis of α-β phase heterojunction on Bi_2O_3 nanowires with exceptional visible-light photocatalytic performance, *Applied CatalysisB: Environmental* , 142–143, 504, **2013**.

[25] Anthony R. West, *Solid State Chemistry and its Application*, Wiley, New York, **1984.**

[26] H.F. Cheng, B.B. Huang, J.B. Lu, Z.Y. Wang, B. Xu, X.Y. Qin, X.Y. Zhang, Y. Dai, Synergistic effect of crystal and electronic structures on the visible-light-driven photocatalytic performances of Bi_2O_3 polymorphs , *Physical Chemistry Chemical Physics*, 12, 47, 15468, **2010**.

[27] Karvaly B, Hevesi I. Z, Investigations on Diffuse Reflectance Spectra of V_2O_5 Powder , *Naturforsch* A , 26, 245, **1971**.

[28] G. Newcombe, R. Hayes, M. Dribas, Granular activated carbon: Importance of surface properties in the adsorption of naturally occurring organics, *Colloids and Surfaces A: Physicochemical and Engineering Aspects* , 78, 65, **1993**.

[29] S. Sakthivel, B. Neppolian, M.V. Shankar, B. Arabindoo, M. Palanichamy, V. Murugesan, Solar photocatalytic degradation of azo dye: comparison of photocatalytic efficiency of ZnO and TiO_2 , Solar Energy Materials and Solar Cells, 77, 1, 65, **2003**.

[30] C. Lizama, J. Freer, J. Baeza, H.D. Mansilla, Optimized photodegradation of Reactive Blue 19 on TiO_2 and ZnO suspensions, *Catalysis Today*, 76, 2-4, 235, **2002**.

[31] N. Daneshvar, D. Salari, A.R. Khataee, Photocatalytic degradation of azo dye acid red 14 in water on ZnO as an alternative catalyst to TiO_2, *Journal of Photochemistry and Photobiology A: Chemistry* , 162, 2-3, 317, **2004**.

[32] M. Munner, D. bahnemann, Semiconductor-mediated photocatalyzed degradation of two selected pesticide derivatives, terbacil and 2, 4, 5-tribromoimidazole, in aqueous suspension , *Applied Catalysis B: Environmental* , 36, 2, 95, **2002**.

[33] T. Velegraki, I. Poulios, M. Charalabaki, N. kalogerakis, P. Samaras, D. Mantzavinos, Photocatalytic and sonolytic oxidation of acid orange 7 in aqueous solution , Applied Catalysis B: Environmental, 62, 1-2, 159, **2006**.

[34] K. Okamoto, Y. Yamamoto, H. Tanaka, M. Hanaka, A. Itaya, Kinetics of Heterogeneous Photocatalytic Decomposition of Phenol over Anatase TiO_2 Powder, *Bulletin of Chemical Society of Japan* , 58, 7, 2023, **1985**.

[35] M.S.T. Goncalves, A.M.F. Oliveira-Compos, E.M.M.S. Pinto, P.M.S.Plasencia, M.J.R.P. Queiroz, Photochemical treatment of solutions of azo dyes containing TiO_2, *Chemosphere* , 39, 5, 781, **1999**.

[36] S. Chakrabarti, B.K. Dutta, Photocatalytic degradation of model textile dyes in wastewater using ZnO as semiconductor catalyst, *Journal of Hazardous Materials* , 112, 3, 269, **2004**.

[37] N. Sobana, M. Swaminathan, The effect of operational parameters on the photocatalytic degradation of acid red 18 by ZnO , *Separation and Purification Technology*, 56, 1, 101, **2007**.

[38] R.W. Matthews, Photooxidation of organic impurities in water using thin films of titanium dioxide, *Journal of Physical Chemistry* , 91, 3328, **1987**.

[39] I. Poulios, I. Aetopoulou, Photocatalytic degradation of the textile dye reactive orange 16 in the presence of TiO_2 suspensions, *Environmental Technology*, 20, 5, 479, **1999**.

[40] N. San, A. Hatipoglu, G. Kocturk, Z. Cinar, Prediction of primary intermediates and the photodegradation kinetics of 3-aminophenol in aqueous TiO_2 suspensions, *Journal of Photochemistry and Photobiology A: Chemistry* , 139, 2-3, 225, **2001**.

[41] A. Mills, R.H. Davis, D. Worsely, Water purification by semiconductor photocatalysis, *Chemical Society Reviews,* 22, 6, 417, **1993**.

[42] N.A. Laoufi, D. Tassalit, F. Bentahar, The degradation of phenol in water solution by TiO2 photocatalysis in a helical reactor, *Global NEST Journal*, 10, 404, **2008**.

[43] C.S. Turchi, D.F. Ollis, Photocatalytic degradation of organic water contaminants: mechanisms involving hydroxyl radical attack , *Journal of Catalysis,* 122, 1, 178, **1990**.

[44] A.V. Emeline, V. Ryabchuk, N. Serjone, Factors affecting the efficiency of a photocatalyzed process in aqueous metal-oxide dispersions: Prospect of distinguishing between two kinetic models , *Journal of Photochemistry and Photobiology A: Chemistry* , 133, 1-2, 89, **2000**.

6. ACKNOWLEDGEMENTS

The corresponding author Mohamed BADAOUI would like to thank the People's Democratic Republic of Algeria, for her help, and thanks Prof F.J.Beltrán for his help. We would like to thank the Department of Chemical Engineering and Physical Chemistry, Universitydad Extremadura Badajoz, Spain for the synthesis and characterizations.